Extreme Mechanics Letters 48 (2021) 101434

Contents lists available at ScienceDirect

Extreme Mechanics Letters

journal homepage: www.elsevier.com/locate/eml

Fatigue-resistant polyurethane elastomer composites

Guogao Zhang [a,b,1], Tenghao Yin [a,c,1], Guodong Nian [a], Zhigang Suo [a,*]

[a] John A. Paulson School of Engineering and Applied Sciences, Kavli Institute for Bionano Science and Technology, Harvard University, MA, 02138, USA
[b] State Key Laboratory of Chemical Engineering, College of Chemical and Biological Engineering, Zhejiang University, Hangzhou 310027, China
[c] State Key Laboratory of Fluid Power & Mechatronic System, Key Laboratory of Soft Machines and Smart Devices of Zhejiang Province, Center for X-Mechanics, and Department of Engineering Mechanics, Zhejiang University, Hangzhou 310027, China

ARTICLE INFO

Article history:
Received 22 May 2021
Accepted 8 July 2021
Available online 14 July 2021

Keywords:
Polyurethane elastomer
Composite
Toughness
Adhesion
Fatigue threshold

ABSTRACT

Polyurethane (PU) elastomers are among the most used rubberlike materials due to their combined merits, including high abrasion resistance, excellent mechanical properties, biocompatibility, and good processing performance. A PU elastomer exhibits pronounced hysteresis, leading to a high toughness on the order of 10^4 J/m^2. However, toughness gained from hysteresis is ineffective to resist crack growth under cyclic load, causing a fatigue threshold below 100 J/m^2. Here we report a fatigue-resistant PU fiber–matrix composite, using commercially available Spandex as the fibers and PU elastomer as the matrix. The Spandex fibers are stiff, strong, and stretchable. The matrix is soft, tough, and stretchable. We describe a pullout test to measure the adhesion toughness between the fiber and matrix. The test is highly reproducible, showing an adhesion toughness of 3170 J/m^2. The composite shows a maximum stretchability of 6.0, a toughness of 16.7 kJ/m^2, and a fatigue threshold of 3900 J/m^2. When a composite with a precut crack is stretched, the soft matrix causes the crack tip to blunt greatly, which distributes high stress over a long segment of the Spandex fiber ahead the crack tip. This deconcentration of stress makes the composite resist the growth of cracks under monotonic and cyclic loads. The PU elastomer composites open doors for realistic applications of fatigue-resistant elastomers.

1. Introduction

Polyurethanes (PUs) have been developed since the first discovery of Otto Bayer in 1937 [1–4]. PUs are widely used in various foams, elastomers, adhesives, plastics, and fibers [1–9]. Among them, elastomers count about 15% [4]. PU elastomers show superior properties, including high abrasion resistance, excellent mechanical properties, biocompatibility, and easy processing [10–17].

The mechanical properties of PU elastomers have been extensively studied, and are found to be highly related to their microphase-separated structures [11–13]. PU elastomers are composed of hard segments and soft segments. The chemical dissimilarity results in the microphase separation between the hard domains and soft domains, which are linked together by both covalent and hydrogen bonds [11].

In a load-bearing application, an elastomer is commonly required to resist both monotonic and cyclic stretch, characterized by two material properties: toughness and fatigue threshold. The uniformly distributed hard domains of PU serve as toughners, dissipating energy during deformation, and resulting in a high toughness [12]. However, toughness gained from energy dissipation is ineffective to resist crack growth under cyclic stretch, causing a low fatigue threshold of PU elastomer (below 100 J/m^2) [18,19]. In fact, the fatigue threshold of all existing commercial elastomers is much lower than their toughness (Fig. 1). Increasing the fatigue threshold can prevent the propagation of crack, and largely elongate the product lifetime. The low fatigue threshold of polymeric elastomers has been well predicted by the Lake–Thomas model, but increasing the fatigue threshold still remains a challenge [18].

It has been demonstrated that fatigue threshold is greatly amplified in elastomer composites [21–23]. However, fibers used in these works are made from either PDMS or hydrogels, which are not widely applied in industry. Here, we show that Spandex, which is also a PU, can be used as fibers to design fatigue-resistant elastomers. Spandex is a synthetic fiber well known for its exceptional stretchability and strength [24]. Using pullout tests, we will show that the Spandex fibers have good adhesion with the PU matrix. The composite shows a stretchability of 6.0, a toughness of 16.7 kJ/m^2, and a fatigue threshold of 3900 J/m^2. The fatigue threshold is the highest among all the existing elastomers (Fig. 1).

* Corresponding author.
E-mail address: suo@seas.harvard.edu (Z. Suo).
[1] These authors contributed equally to this work.

https://doi.org/10.1016/j.eml.2021.101434
2352-4316/

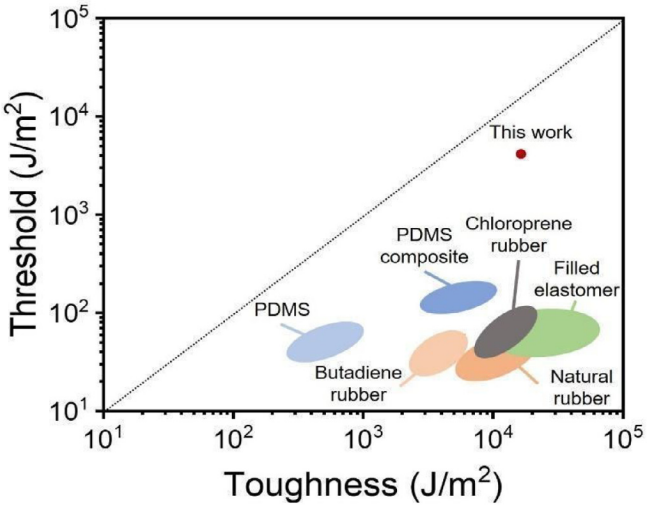

Fig. 1. The polyurethane composite of this work is compared with various other elastomers on the plane of toughness and fatigue threshold. Data of various other elastomers are collected from [20,21].

2. Results and discussion

We start with the preparation of the composite. PUs are usually classified into thermoplastic polyurethane (TPU) and thermoset PU [10,11]. TPUs are often produced in pellets and processed through injection molding, whereas thermoset PUs are often made from liquid precursors and cured by heat or by mixing with a catalyst. We choose a thermoset PU elastomer for easy manipulation in the lab. The thermoset PU elastomer comes with a two-component reactive liquid precursor, part A (a mixture of toluene diisocyanates) and part B (a mixture of polyols). The thermoset PU elastomer can be cured through the reaction between isocyanate groups from the toluene diisocyanates and hydroxyl groups from the polyols. The processing is conducted following the product instruction. A mold with an open spacer ($100 \times 120 \times 2.4$ mm^3) is made from silicon rubber, and Spandex fibers are aligned in parallel every 10 mm in the mold. Part A and Part B of equal weight are mixed thoroughly and degassed. The mixture is poured into the mold. After degassing in vacuum, the mixture is cured at 65 °C overnight (Fig. 2a). Pure PU elastomers are prepared in the same way, but without Spandex fibers in mold. Each Spandex fiber consists of many smaller individual fibers that adhere to each other, with pores between them [24]. The cross-section photo of the composite shows a full contact between a Spandex fiber and the PU matrix (Fig. 2b). The mixture does not penetrate into the inner pores of the fibers even with vacuum treatment.

Mechanical measurements are performed using a tensile tester (Instron5966) with a load cell of 100N for Spandex fiber tests and pullout tests, and 10 kN for other tests. All samples in this work are loaded at a constant rate of 5 mm/s at room temperature. Pure elastomer samples and the composite samples are glued between two rigid plastic grippers using crazy glue (406^{TM}, Henkel Loctite). In the undeformed state, the stretchable part of each sample is of length $L = 100$ mm, thickness $t = 2.1$ mm, and height $H = 10$ mm. Thin sheet tests are conducted on the PU matrix (Fig. 3a) and the composite (Fig. 3c). Uniaxial tensile test is conducted on Spandex fibers (Fig. 3b). All samples are stretched to fracture. The maximum stretch is 7.0 for Spandex fiber and 9.4 for the PU matrix. The comparable maximum stretches guarantee the high stretchability of the composite. The modulus of the PU matrix and Spandex fiber is 0.18 MPa and 1.38 MPa, respectively. The composite has a modulus of 0.24 MPa (Table 1). Cyclic load tests at various maximum stretches are performed to determine the hysteresis of the PU matrix (Fig. 3d), Spandex fiber (Fig. 3e), and the composite (Fig. 3f). The significant hysteresis of these samples comes from the plastic deformation of the hard segments in the PU polymers [12,25,26]. In previous works on elastomer composites, the adhesion between two elastomers is measured by peel [21,23]. This test requires a bi-elastomer sample, and is unsuitable here because Spandex fibers are used. Here we develop a pullout test to study the adhesion between the fiber and matrix (Fig. 4, SI Move 1). We fabricate a sample by casting the matrix around a single fiber, following the procedure described above. The upper part of the sample is glued between two rigid plastic plates, which are locked to the upper arm of the tester, with no pressure applied to the sample. The lower part of the sample is pressed by the clamps and fixed to the lower arm of the tester. The PU matrix is cut along the edge of the upper gripper, and only a small amount of matrix is left around the fiber. The sample is pulled monotonically. The force–displacement curves exhibit five distinct stages (Fig. 4b,c). In the reference state, both the displacement and force are zero (I). During load, both the fiber and surrounding matrix are stretched, and the force increases to a peak (II). At the peak, the surrounding matrix ruptures, the fiber is intact but a debond sets in, and the force drops drastically (III). As the displacement further increases, the debond advances in a steady state, and the force settles on a plateau (IV). Finally, the debond reaches the end of the fiber, the fiber pulls out completely, and the force vanishes (V). The debond front is marked by red arrows in the snapshots of the pullout process.

Table 1
Summary of the mechanical properties of pure PU, Spandex fiber, and the composite.

Sample	Modulus (MPa)	Maximum stretch	Work of fracture (MJ/m^3)	Toughness (kJ/m^2)
Pure PU	0.18	9.4	7.1	11.5
Spandex fiber	1.38	7.0	71.1	–
Composite	0.24	6.0	4.1	16.7

We repeat this experiment multiple times (Fig. 5). The peak force varies from sample to sample, corresponding to the sudden rupture of the surrounding matrix and the nucleation of the debond between the fiber and matrix. The variation in the peak force is likely caused by the sharpness of the cut and the amount of leftover matrix surrounding the fiber, and both are not well controlled. The process of the large drop in force is complicated, and will not be studied in this work. The plateau force, however, is highly reproducible, corresponding to the steady advance of the debond front. We will use this plateau force to characterize the adhesion between the fiber and matrix.

Pullout tests are commonly conducted in developing stiff composites, in which deformation is small [27]. In our pullout test, however, the deformation of the Spandex fiber is large before the debond sets in. We now model the steady-state pullout by including the large deformation of the fiber (Fig. 4a). In the reference state, let D be the diameter of the fiber, and L be the debond length. In a current state, let l be the length of the free part of the fiber, and F be the applied force. The stretch of the fiber is $\lambda = l/L$, and the nominal stress of the fiber is $s = 4F/\pi D^2$. Let $W(\lambda)$ be the free energy per unit volume of the fiber. Recall that $dW = s\,d\lambda$, so that $W(\lambda)$ is the area under the stress–stretch curve of the fiber (Fig. 3b).

The fiber, the applied force, and the matrix constitute a thermal system, which exchanges energy with the surroundings by heat, but its temperature is taken to be constant. In the steady state, both the force F and stretch λ are constant. When the

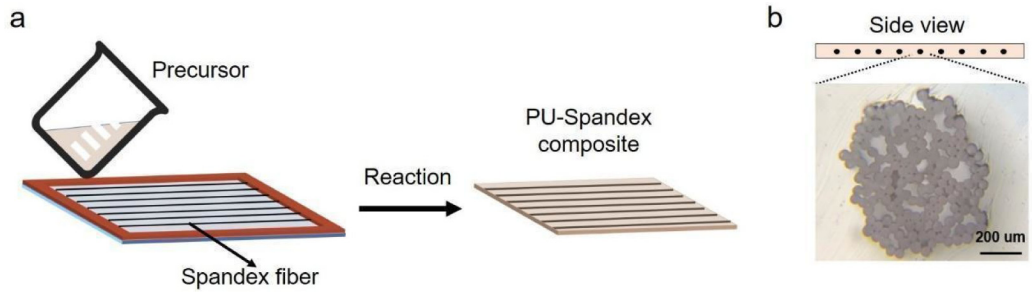

Fig. 2. (a) Preparation of the polyurethane composite. (b) Micrograph of a cross-section.

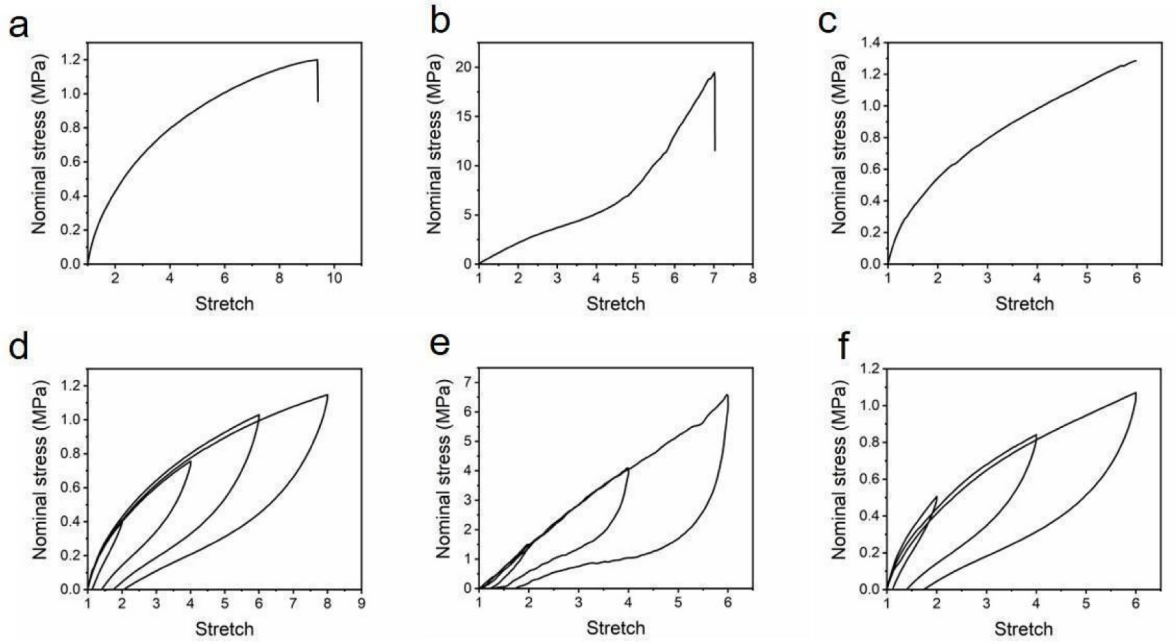

Fig. 3. Stress–stretch curves under monotonic and cyclic load of (a, d) the PU matrix, (b, e) Spandex fiber, and (c, f) the composite.

debond front advances, the matrix near the bonded fiber also deforms, and the fields travel with the debond front in a steady state. Because the matrix is much softer than the fiber, here we neglect the change in the elastic energy in the matrix. The volume of the matrix is much larger than that of fiber, so that the fiber ahead of the debond front deforms negligibly. Consequently, the free energy of this thermal system consists of the free energy of the fiber and the applied force:

$$\Pi(F, L) = \frac{\pi D^2}{4} LW(\lambda) - F(\lambda - 1)L \tag{1}$$

The energy release rate G is defined as the reduction in the free energy of the thermal system associated with the debond advancing per unit area:

$$G = -\frac{\partial \Pi(F, L)}{\partial(\pi DL)} \tag{2}$$

We find that

$$G = \frac{F(\lambda - 1)}{\pi D} - \frac{D}{4} W(\lambda) \tag{3}$$

When the debond advances in a steady state, the energy release rate G attains the adhesion toughness. We read the plateau force F from the pullout force–displacement diagram (Fig. 5), calculate the nominal stress s, and read the stretch λ from the stress–stretch curve of the fiber (Fig. 3b). The diameter of the fiber in the reference state D can be measured by microscope in the experiment. The free energy $W(\lambda)$ can be obtained by integrating the stress–stretch curve of the fiber from 1 to λ. We obtain that $F = 2.11 \pm 0.06$ N, $\lambda = 5.37 \pm 0.05$, $D = 0.53$ mm, and $W(\lambda) = 17.87 \pm 0.47$ MJ/m^3. The calculated adhesion toughness is 3169.7 ± 168.7 J/m^2. This high adhesion toughness is likely caused by topological entanglements of the freshly formed PU elastomer with the polymer network of the Spandex fiber.

We show the fracture process of the composite with a precut crack under monotonic load. We calculate the nominal stress using the applied force divided by the cross-sectional area in the undeformed state of the uncut sample, and mark five states on the measured stress–stretch curve (Fig. 6a). First, the sample is undeformed (Fig. 6b). Upon load, the crack propagates from the initial length to the first fiber (Fig. 6c). Then, debond happens between the fiber and the matrix, which causes the crack to bypass the first fiber and comes to the next fiber (Fig. 6d). The debond causes a drop in the measured stress. The propagation-debond process repeats (Fig. 6e) until the crack goes through the whole sample (Fig. 6f). In this test, the crack bypasses the first several fibers but breaks the last several fibers. This phenomenon is quite stable in the repeated tests.

Toughness is measured using a thin sheet test [23,28]. Briefly, two samples are prepared with the same dimensions ($100 \times 10 \times 2.1$ mm^3). An edge precut crack is introduced to one sample, and the other remains intact. Both samples are subjected to monotonic load. The toughness is given by $W(\lambda_c)H$, where λ_c

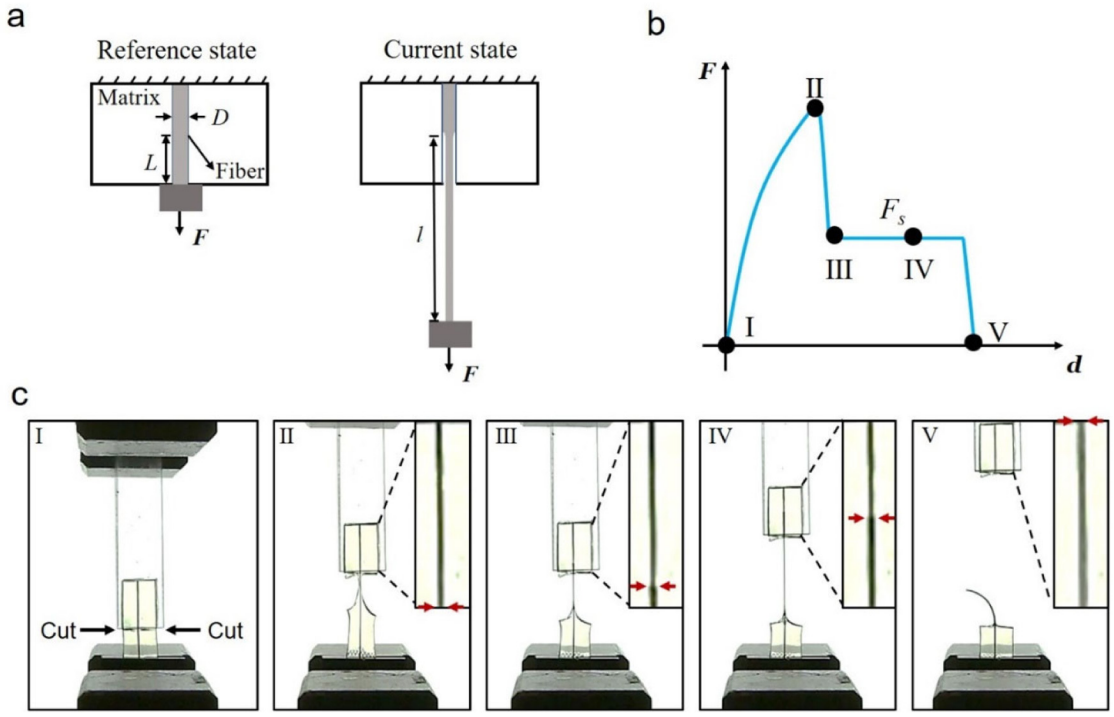

Fig. 4. Pullout test. (a) Schematic of pullout. (b) Schematic of the force–displacement curve marked with five states: zero displacement (I), maximum force (II), initial debond (III), steady-state debond (IV), and complete pullout (V). (c) The corresponding snapshots during the pullout process. The inset shows the debond front with red arrows.. (For interpretation of the references to color in this figure legend, the reader is referred to the web version of this article.)

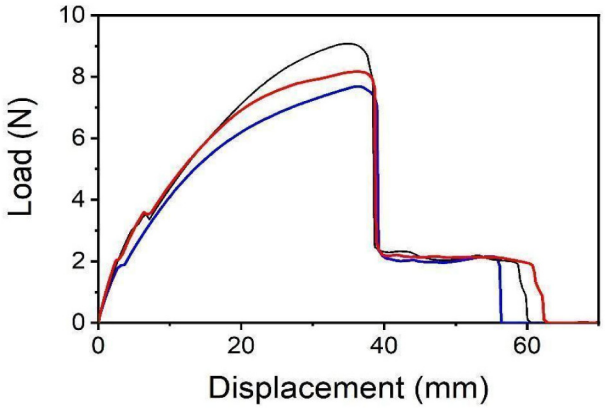

Fig. 5. Force–displacement curves of pullout of three samples.

is the stretch of the precut sample when the crack bypasses the first fiber, $W(\lambda_c)$ is the corresponding area underneath the stress–stretch curve of the uncut sample, and H is the height of the sample in the reference state. The measured toughness of the composite is ∼16.7 kJ/m^2. By contrast, the toughness of pure PU is ∼11.5 kJ/m^2 (Table 1). This increase of toughness can be understood by the concept of stress-deconcentration as follows [22,23,29]. When the crack tip reaches the fiber, the stress distributes along the fiber, releasing the stress concentration at the crack tip. Though debond happens between the fiber and matrix, making the crack bypass the fiber, the deconcentration of the stress makes the energy required to grow the crack larger.

Cyclic thin-sheet tests have been developed by Thomas A. G. and others to study the fatigue crack propagation of elastomers [21,30,31]. We conduct a cyclic load test on the composites. An edge precut crack is introduced to the sample with a razor blade. The sample is then loaded on the machine. We prescribe a maximum stretch λ in each load cycle. Stress–stretch curves are recorded by the machine, and the crack length is monitored by a camera. Fig. 7a shows the crack growth process of the composite. The sample is subjected to a cyclic load with a maximum stretch of 2.3. It takes 1035 cycles for the crack to propagate to the first fiber and another 3861 cycles to cross the first fiber. The slow-down of the crack propagation is again due to the stress deconcentration.

Since the composite has a significant hysteresis (Fig. 3f), the stress–stretch curve during cyclic load keeps shaking down and then remains nearly unchanged. We determine the energy release rate G according to our previous work [32]. Briefly, the energy release rate G is calculated through the equation $G = W(\lambda)H$, where H is the height of the sample in the undeformed state, and $W(\lambda)$ is the area underneath the steady-state stress–stretch curve of the sample without a precut, with the prescribed stretch λ. In this work, we obtain the steady-state stress–stretch curve after 100 cycles. The failure of the sample is recognized when the crack bypasses the first fiber [21]. We reduce the applied maximum stretch for different samples until the crack cannot bypass the first fiber after 20,000 cycles. The applied stretch λ is set to 4, 3, 2.3, 2.1. The calculated energy release rate G and corresponding failure cycle number N are plotted in Fig. 7b. The number of cycles to failure increases when G decreases. When G is ∼3900 J/m^2, the crack does not bypass the first fiber after 20,000 cycles. Thus, 3900 J/m^2 is regarded as the fatigue threshold of the composite.

The fiber–matrix design for enhancement of the elastomer threshold has been explored in our previous works [21–23]. There are four design principles: (i) the matrix is much softer than the fiber, (ii) the adhesion between the matrix and the fiber is strong, (iii) the matrix should be resistant to large shear deformation, and (iv) the fiber diameter should be large enough. When the crack passes through the matrix and comes to the fiber, the hard fiber blocks the propagation of the crack. At the same time, the soft matrix undergoes large shear deformation and alleviates the

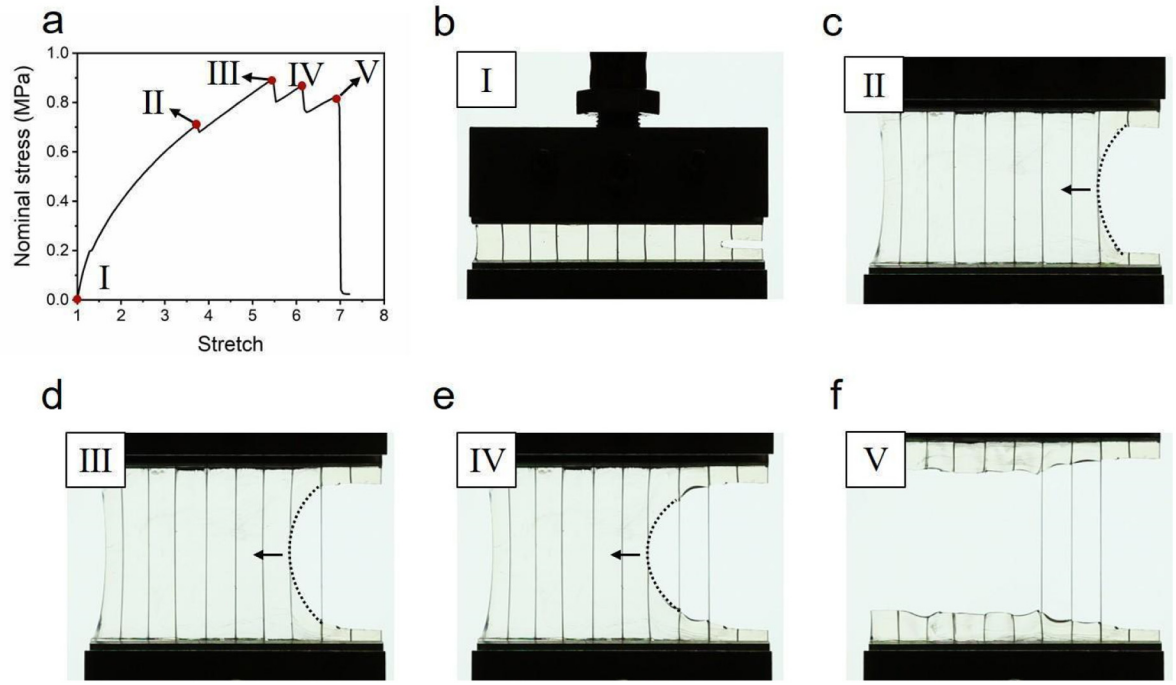

Fig. 6. Fracture process of a composite under monotonic load. (a) Stress–stretch curve of a precut sample marked with five states. (b–f) Photos of the five states.

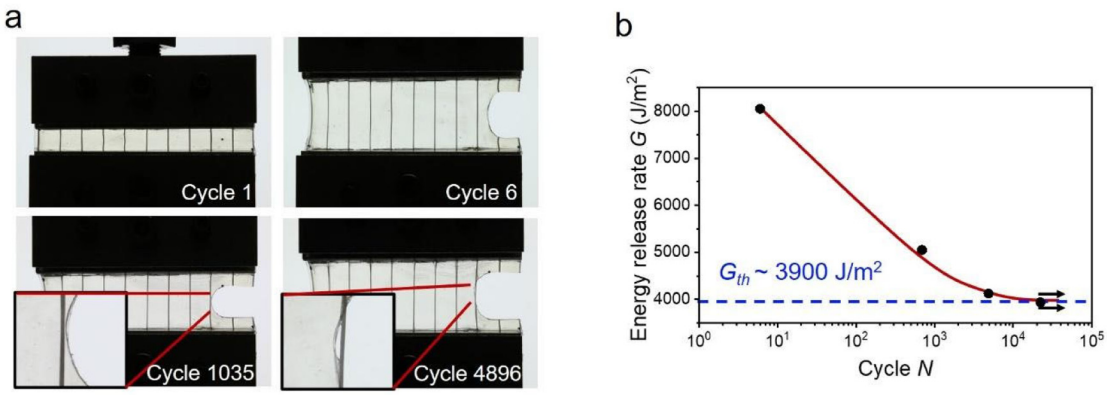

Fig. 7. Fatigue test of the composite. (a) Photos of the composite at various cycles of load. The amplitude of energy release rate is 4124 J/m^2. The insets show the crack tip before and after passing the first fiber. (b) At a prescribed amplitude of energy release rate G, the number of cycles N is recorded when the precut crack passes the first fiber. The fatigue threshold (∼3900 J/m^2) is obtained when no crack growth can be detected after 20,000 cycles.

stress concentration in the fiber. The adhesion between matrix and fiber plays an important role. Strong adhesion binds the fiber and the matrix. The threshold of ∼3900 J/m^2 is the highest among all the existing elastomers.

3. Conclusions

In this work, we demonstrate a fatigue-resistant elastomer made from commercially available Spandex fibers and PU matrix, through a fiber–matrix composite design. The obtained composite shows a large stretchability of 6.0, toughness of 16.7 kJ/m^2, and fatigue threshold of 3900 J/m^2. The adhesion toughness between Spandex fiber and PU matrix is 3170 J/m^2. The high fatigue threshold and toughness benefit from the fiber–matrix composite design and the good adhesion. The pullout tests are highly stable, showing the potential to be extended to other fiber–matrix composite systems. The composite is made from commercially available materials, which can readily find immediate applications on fatigue-resistant elastomers.

Declaration of competing interest

The authors declare that they have no known competing financial interests or personal relationships that could have appeared to influence the work reported in this paper.

Acknowledgments

G. Zhang was supported by the Office of China Postdoctoral Council as a postdoctoral fellow at Harvard University. T. Yin was supported by the China Scholarship Council as a visiting scholar at Harvard University. The work at Harvard was supported by the Air Force Office of Scientific Research, USA under award number FA9550-20-1-0397, and by the National Science Foundation, USA through the Harvard University Materials Research Science and Engineering Center DMR-2011754.

Appendix A. Experimental section

Preparation of PU-Spandex composite

The PU precursor (VytaFlex® 20) is purchased from Smooth-On company. Spandex fibers with the trading name of Dorlastan (dtex 1870 v550 1680 den) and silicon rubber sheets with a thickness of 2.4 mm are purchased from McMaster. Spandex fibers are cleaned with oxygen plasma (Plasma Prep2, GALA Instrument) for 10 s at a power of 30 W before use. The silicon rubber is used to make a mold with an open spacer ($100 \times 120 \times 2.4$ mm^3), and Spandex fibers are aligned parallelly every 10 mm in the mold.

Part A and part B of the PU precursor are mixed by a weight ratio of 1:1 thoroughly using a mixer (Thinky ARE-300) at 2000 r/min for one minute, and then degas at 2000 r/min for another minute. Typically, 28 g of the mixer is poured into the spacer and further degassed in vacuum (<0.01 torr) for 10 mins. The precursor is cured in an oven at 65 °C overnight. After that, the cured composite film is peeled off from the mold. The preparation of pure PU samples is the same as above but without Spandex fibers. The obtained composite and the pure PU are cut into a rectangular shape ($100 \times 40 \times 2.1$ mm^3, long length perpendicular to the fiber) for further test. The diameter of the Spandex fiber is ∼0.53 mm. The volume fraction of the Spandex fibers in the composite is estimated by volume calculation to be ∼0.09%.

Optical microscope

All the optical microscopic pictures are taken using a Nikon AZ100 microscope. The composite is cut into thin slices for microscope observation. The diameter of Spandex fiber is obtained from the cross-section photo of the composite.

Mechanical tests

The Spandex samples are prepared as a single fiber with both ends fixed on the clamps, and the initial length of the sample is recorded. The shear modulus of the fiber is calculated as one-third the initial slope of the stress–stretch curve measured by uniaxial tension test. The shear moduli of the PU and the composite are calculated as one-fourth the initial slope of the stress–stretch curve measured by thin sheet test. In the hysteresis tests, the load–unload curves with different maximum stretches are obtained from different samples. For all samples with a precut, the length of the precut is ∼10 mm.

Pullout tests

The composites are cut into rectangular shapes ($10 \times 40 \times 2.1$ mm^3). The upper part of the sample is glued between two rigid plastic grippers (the glued length is 15 mm out of 40 mm), and the grippers are fixed at the clamp of the stretching machine without pressure on the sample. The other end of the sample is fixed by the clamp, and the fixed-length is about 15 mm. Samples are cut at the edge of the upper gripper to expose the Spandex fiber. Samples are stretched until the entire fiber in the gripper is pulled out.

Appendix B. Supplementary data

Supplementary material related to this article can be found online at https://doi.org/10.1016/j.eml.2021.101434.

References

[1] H.W. Engels, H.G. Pirkl, R. Albers, R.W. Albach, J. Krause, A. Hoffmann, H. Casselmann, J. Dormish, Polyurethanes: versatile materials and sustainable problem solvers for today's challenges, Angew. Chem. Int. Ed. 52 (2013) 9422–9441.
[2] M. Szycher, Szycher's Handbook of Polyurethanes, CRC press, 1999.
[3] J.O. Akindoyo, M.D.H. Beg, S. Ghazali, M.R. Islam, N. Jeyaratnam, A.R. Yuvaraj, Polyurethane types, synthesis and applications – a review, RSC Adv. 6 (2016) 114453-114482.
[4] M.F. Sonnenschein, Polyurethanes: Science, Technology, Markets, and Trends, John Wiley & Sons, 2014.
[5] M.M. Demir, I. Yilgor, E. Yilgor, B. Erman, Electrospinning of polyurethane fibers, Polymer 43 (2002) 3303–3309.
[6] P. Jain, T. Pradeep, Potential of silver nanoparticle-coated polyurethane foam as an antibacterial water filter, Biotechnol. Bioeng. 90 (2005) 59–63.
[7] D. Dieterich, O. Bayer, Polyurethane plastics, 1969, U.S. Patents No. 3479310.
[8] M.A. Osman, V. Mittal, M. Morbidelli, U.W.J.M. Suter, Polyurethane adhesive nanocomposites as gas permeation barrier, Macromolecules 36 (2003) 9851–9858.
[9] G.W. De Santis, Polyurethane sealant-primer system isocyanate-reactive surface primer composition for polyurethane sealants, 1972, U.S. Patents No. 3707521.
[10] I. Clemitson, Castable Polyurethane Elastomers, CRC Press, 2015.
[11] C. Hepburn, Polyurethane Elastomers, Springer Science & Business Media, 2012.
[12] Z.S. Petrović, J. Ferguson, Polyurethane elastomers, Prog. Polym. Sci. 16 (1991) 695–836.
[13] C. Prisacariu, Polyurethane Elastomers: From Morphology to Mechanical Aspects, Springer Science & Business Media, 2011.
[14] L.W. McKeen, Thermoplastic Elastomers, William Andrew, 2016.
[15] M. Szycher, Biostability of polyurethane elastomers: a critical review, J. Biomater. Appl. 3 (1988) 297–402.
[16] G.T. Howard, Biodegradation of polyurethane: a review, Int. Biodeter. Biodegr. 49 (2002) 245–252.
[17] K. Stokes, R. McVenes, J.M. Anderson, Polyurethane elastomer biostability, J. Biomater. Appl. 9 (1995) 321–354.
[18] G.J. Lake, A.G. Thomas, D. Tabor, The strength of highly elastic materials, P. Roy. Soc. A-Math. Phys. 300 (1967) 108–119.
[19] H.K. Mueller, W.G. Knauss, The fracture energy and some mechanical properties of a polyurethane elastomer, Tran. Soc. Rheol. 15 (1971) 217–233.
[20] N.A. Fleck, K.J. Kang, M.F. Ashby, Overview no 112: The cyclic properties of engineering materials, Acta Metall. Mater. 42 (1994) 365–381.
[21] C. Li, H. Yang, Z. Suo, J. Tang, Fatigue-resistant elastomers, J. Mech. Phys. Solids 134 (2020) 103751.
[22] C. Xiang, Z. Wang, C. Yang, X. Yao, Y. Wang, Z. Suo, Stretchable and fatigue-resistant materials, Mater. Today (2019) 7–16.
[23] Z. Wang, C. Xiang, X. Yao, P. Le Floch, J. Mendez, Z. Suo, Stretchable materials of high toughness and low hysteresis, Proc. Natl. Acad. Sci. 116 (2019) 5967–5972.
[24] T. Nakajima, K. Kajiwara, J.E. McIntyre, Advanced Fiber Spinning Technology, Woodhead Publishing, 1994.
[25] H.J. Qi, M.C. Boyce, Stress–strain behavior of thermoplastic polyurethanes, Mech. Mater. 37 (2005) 817–839.
[26] J. Yi, M.C. Boyce, G.F. Lee, E. Balizer, Large deformation rate-dependent stress–strain behavior of polyurea and polyurethanes, Polymer 47 (2006) 319–329.
[27] P.S. Chua, M.R. Piggott, The glass fibre—polymer interface: I—theoretical consideration for single fibre pull-out tests, Compos. Sci. Technol. 22 (1985) 33–42.
[28] J.Y. Sun, X. Zhao, W.R. Illeperuma, O. Chaudhuri, K.H. Oh, D.J. Mooney, J.J. Vlassak, Z. Suo, Highly stretchable and tough hydrogels, Nature 489 (2012) 133–136.
[29] J. Liu, C. Yang, T. Yin, Z. Wang, S. Qu, Z. Suo, Polyacrylamide hydrogels. II. elastic dissipater, J. Mech. Phys. Solids 133 (2019) 103737.
[30] A.G. Thomas, Rupture of rubber. V., Rupture of rubber. v cut growth in natural rubber vulcanizates, J. Poly. Sci. 31 (1958) 467–480.
[31] J. Tang, J. Li, J.J. Vlassak, Z. Suo, Fatigue fracture of hydrogels, Extreme Mech. Lett. 10 (2017) 24–31.
[32] R. Bai, Q. Yang, J. Tang, X.P. Morelle, J. Vlassak, Z. Suo, Fatigue fracture of tough hydrogels, Extreme Mech. Lett. 15 (2017) 91–96.